

## Two Wheel Speed Robust Sliding Mode Control for Electric Vehicle Drive

Abdelfatah Nasri<sup>1</sup>, Abdeldjebar Hazzab<sup>1</sup>,  
Ismail K. Bousserhane<sup>1</sup>, Samir Hadjeri<sup>2</sup>, Pierre Sicard<sup>3</sup>

**Abstract:** Nowadays the uses of electrical power resources are integrated in the modern vehicle motion traction chain so new technologies allow the development of electric vehicles (EV) by means of static converters-related electric motors. All mechanical transmission devices are eliminated and vehicle wheel motion can be controlled by means of power electronics. The proposed propulsing system consists of two induction motors (IM) that ensure the drive of the two back driving wheels. The proposed control structure-called independent machines- for speed control permit the achievement of an electronic differential. The electronic differential system ensures the robust control of the vehicle behavior on the road. It also allows controlling, independently, every driving wheel to turn at different speeds in any curve. This paper presents the study and the sliding mode control strategy of the electric vehicle driving wheels.

**Keywords:** Electric vehicle, Electronic differential, Induction machine, Driving wheels, Sliding mode control, Multi-converters multi-machines systems.

### 1 Introduction

The major technological progress for the mechanic vehicles is either partial or total introduction of electricity into motorization thereof, and in the electric traction system. This is can be provided by the technology of power converters integration, the energy storage in the batteries and the development of super-condensers.

Some applications in the field of electrical drives require the use of several electric machines and as well as many static converters that play an important part among the electro-mechanic systems. These systems are called multi-converters/multi-machines systems (MCMMS) [1]. They are recognized through the existence of the coupling system type, either electric or magnetic or mechanical in nature, used in several electric machines propulsing the vehicle. Here, as a control, we model the coupling by using appropriated control

---

<sup>1</sup>University Center of Bechar, B.P 417 Bechar, Algeria, 08000; E-mail: nasriab1978@yahoo.fr

<sup>2</sup>University of Djillali Liabes, BP 98 Sidi Bel-Abbes, Algeria.

<sup>3</sup>Groupe de recherche en électronique industrielle, École d'Ingénierie, Département de Génie électrique et Génie informatique, Université du Québec à, Trois-Rivières, Canada

structures including independent control, average control, or slave master, by imposing criteria of energetic distribution in order to obtain a single machine or a single converter system. One of these control structures can be applied to the control of electric vehicle (EV) driving wheels. Here, we need the models containing the elements constituting the electric traction system. In the sections that follow we shall develop these models.

Nowadays, as the result of intensified progress in power electronics and of micro-computing, the control of the AC electric machines has witnessed a considerable development and the real time implantation applications facilities. AC motors, especially, the induction motor (IM), have several inherent advantages, such as simplicity, reliability, low cost, and almost maintenance-free electrical drives [2]. However, for high dynamic performance in industrial applications, the control thereof remains a challenging problem as they exhibit significant nonlinearities, and many parameters, mainly the rotor resistance, vary by operating conditions. On the other hand, over decades, the direct current machine (DC) constituted the only electromechanical source of variable speed applications owing to its ease of control, whereby torque and flux were naturally decoupled and could be controlled independently by the torque and the flux, both producing current [2,3,6].

Sliding mode control theory, owing to its order reduction, disturbance rejection, strong robustness, and simple implementation by means of the power converter, is one of the prospective control methodologies for electrical machines [6, 7]. The feature of sliding mode control system is that the controller is switched between two distinct control structures. In general, the design of variable structure controller generally includes two steps, i.e. the hitting and the sliding phases [6]. First, when the system is directed towards a switching surface by a feedback control law, the sliding mode occurs. When the system states enter the sliding mode, the dynamics of the system are determined by the selection of the sliding surface. The stated situations are independent of parametric uncertainties and load disturbances. Hence, SMC has been employed for the position and speed control of AC machines.

In this paper, a sliding mode decoupling controller for electric vehicle control is proposed. In addition, an outer-loop speed controller that employs sliding mode control has been derived. The reminder of this paper is as follows: Section 2 reviews the principle components of the electric traction chain accompanied by the equations of the electric vehicle. Section 3 shows the indirect field-oriented control (IFOC) of induction motor. Section 4 shows the development of sliding mode controllers design for electric vehicle. The proposed structure of the studied propulsion system is given in the section 4. Section 5 presents some simulation results of different studied cases. Finally, the conclusion is given in Section 6.

## 2 Electric Traction System Elements Modeling

Fig. 1 represents general diagram of an electric traction system using an induction motor (IM) supplied by voltage inverter [8].

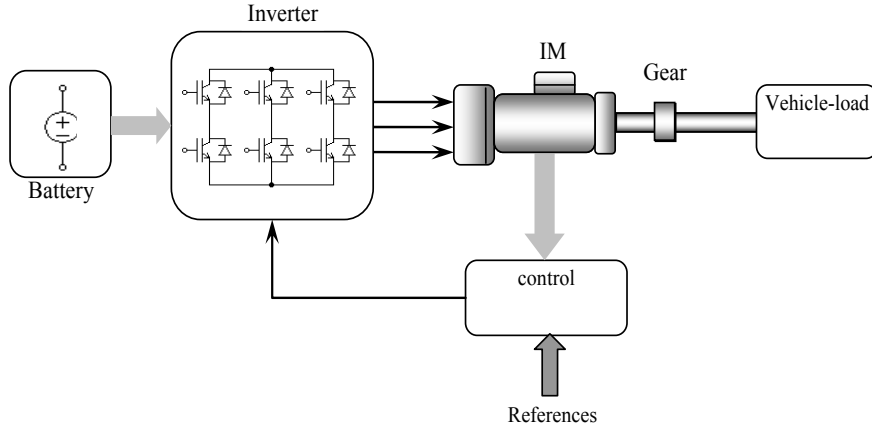


Fig. 1 – Electrical traction chain.

### A. Energy source

The battery considered in this paper is the Lithium-Ion accumulator battery for which a simple model is assumed. Therefore, a simplified version of the complex battery model reported in [9] has been used.

### B. Static converter

In this electric traction system, we use an inverter to obtain three balanced phases of alternating current with variable frequency from the current battery.

$$\begin{bmatrix} v_{an} \\ v_{bn} \\ v_{cn} \end{bmatrix} = \frac{U_{dc}}{2} \begin{bmatrix} 2 & -1 & -1 \\ -1 & 2 & -1 \\ -1 & -1 & 2 \end{bmatrix} \begin{bmatrix} S_a \\ S_b \\ S_c \end{bmatrix}. \quad (1)$$

The logic  $S_i$  of the switches has been obtained by comparing the control signals of the inverter with the modulation signal.

### C. Traction motor

The used motor is a three-phase induction motor type (IM) supplied by a voltage inverter controlled by Pulse Width Modulation (PWM) techniques. A model based on circuit equations is generally sufficient in order to make control synthesis. The dynamic model of three-phase Y-connected induction motor can be expressed in the  $d$ - $q$  synchronously rotating frame as [2, 3, 6]:

$$\left\{ \begin{array}{l} \frac{di_{ds}}{dt} = \frac{1}{\sigma L_s} \left( - \left( R_s + \left( \frac{L_m}{L_r} \right)^2 R_r \right) i_{ds} + \sigma L_s \omega_e i_{qs} + \frac{L_m R_r}{L_r^2} \phi_{dr} + \frac{L_m}{L_r} \phi_{qr} \omega_r + V_{ds} \right) \\ \frac{di_{qs}}{dt} = \frac{1}{\sigma L_s} \left( - \sigma L_s \omega_e i_{ds} - \left( R_s + \left( \frac{L_m}{L_r} \right)^2 R_r \right) i_{qs} - \frac{L_m}{L_r} \phi_{dr} \omega_r + \frac{L_m R_r}{L_r^2} \phi_{qr} + V_{qs} \right) \\ \frac{d\phi_{dr}}{dt} = \frac{L_m R_r}{L_r} i_{ds} - \frac{R_r}{L_r} \phi_{dr} + (\omega_e - \omega_r) \phi_{dr} \\ \frac{d\phi_{qr}}{dt} = \frac{L_m R_r}{L_r} i_{qs} - (\omega_e - \omega_r) \phi_{dr} - \frac{R_r}{L_r} \phi_{qr} \\ \frac{d\omega_r}{dt} = \frac{3 P^2 L_m}{2 L_r J} (i_{qs} \phi_{dr} - i_{ds} \phi_{qr}) - \frac{f_c}{J} \omega_r - \frac{P}{J} T_l \end{array} \right. \quad (2)$$

where  $\sigma$  is the coefficient of dispersion and is given by (2):

$$\sigma = 1 - \frac{L_m^2}{L_s L_r}, \quad (3)$$

$L_s, L_r, L_m$  - stator, rotor and mutual inductances;

$R_s, R_r$  - stator and rotor resistances;

$\omega_e, \omega_r$  - electrical and rotor angular frequency;

$\omega_{sl}$  - slip frequency ( $\omega_e - \omega_r$ );

$\tau_r$  - rotor time constant ( $L_r/R_r$ );

$P$  - pole pairs.

#### D. Mechanical part.

The developed modelling is based on the use of data from the Leroy-Somer Society [4] shown in Fig. 2.

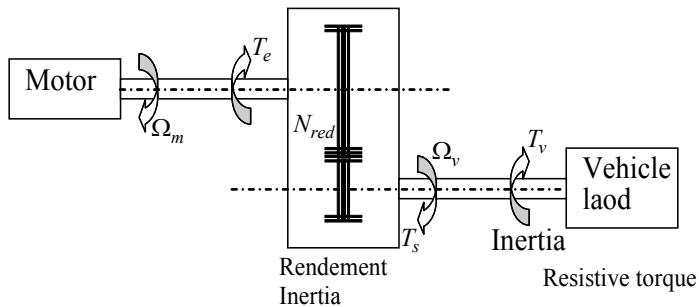


Fig. 2 – Electromechanical structure.

### 1. The vehicle as load

The vehicle considered as a load is characterized by many torques mostly considered as the resistive torque [4, 5, 12, 13, 16, 17].

The vehicle inertia gives a torque defined by the following relationship:

$$T_{in} = J_v \frac{dw_v}{dt} . \quad (4)$$

The aerodynamics torque is:

$$T_{aero} = \frac{1}{2} \rho S T_x R_r^3 w_r^2 . \quad (5)$$

The slope torque is:

$$T_{slope} = Mg \sin \alpha . \quad (6)$$

The maximal torque of the tire which can be opposed to the motion has the following expression:

$$T_{max} = Mgf_r R_r . \quad (7)$$

We obtain finally the total resistive torque:

$$T_v = T_{slope} + T_{tire} + T_{aero} . \quad (8)$$

### 2. Gear

The speed gear ensures the transmission of the motor torque to the driving wheels. The gear is modelled by the gear ratio, the transmission efficiency and its inertia.

The mechanical equation is given by

$$J_e \frac{dw_m}{dt} + fw_m = p(T_{em} - T_r) , \quad (9)$$

$$T_r = \frac{1}{\eta N_{red}} T_v , \quad (10)$$

and

$$J_e = J + \frac{J_v}{\eta N_{red}^2} . \quad (11)$$

The modeling of the traction system allows the implementation of some controls such as the vector control.

### 3 Vector control

The main objective of the vector control of induction motors is to independently control the torque and the flux; this is done by using a  $d-q$  rotating reference frame synchronously with the rotor flux space vector [3, 6]. In ideally

field-oriented control, the rotor flux linkage axis is forced to align with the  $d$ -axes, and it follows that [7, 18, 12, 14]:

$$\varphi_{rq} = \frac{d\varphi_{rq}}{dt} = 0, \quad (12)$$

$$\varphi_{rd} = \varphi_r = \text{constant}. \quad (13)$$

Applying the result of (12) and (13), namely field-oriented control, the torque equation become analogous to the DC machine, and can be described as follows:

$$T_e = \frac{3}{2} \frac{pL_m}{L_r} \varphi_r i_{qs} \quad (14)$$

and the slip frequency can be given as follows:

$$\omega_{sl} = \frac{1}{\tau_r} \frac{i_{qs}^*}{i_{ds}^*}. \quad (15)$$

Consequently, the dynamic equations (1) yield:

$$\frac{di_{ds}}{dt} = -\left(\frac{R_s}{\sigma L_s} + \frac{1-\sigma}{\sigma \tau_r}\right) i_{ds} + \omega_e i_{qs} + \frac{L_m}{\sigma L_s L_r \tau_r} \varphi_{rd} + \frac{1}{\sigma L_s} V_{ds} \quad (16)$$

$$\frac{di_{qs}}{dt} = -\left(\frac{R_s}{\sigma L_s} + \frac{1-\sigma}{\sigma \tau_r}\right) i_{qs} - \omega_e i_{ds} + \frac{L_m}{\sigma L_s L_r \tau_r} \varphi_{rd} + \frac{1}{\sigma L_s} V_{ds} \quad (17)$$

$$\frac{d\varphi_r}{dt} = \frac{L_m}{\tau_r} i_{ds} - \frac{1}{\tau_r} \varphi_{rd} \quad (18)$$

$$\frac{d\omega_r}{dt} = \frac{3}{2} \frac{P^2 L_m}{J L_r} i_{qs} \varphi_{rd} - \frac{f_c}{J} \omega_r - \frac{P}{J} T_l. \quad (19)$$

The decoupling control method with compensation is to choose inverter output voltages such that [10]:

$$V_{ds}^* = \left(K_p + K_i \frac{1}{s}\right) (i_{ds}^* - i_{ds}) - \omega_e \sigma L_s i_{qs}^* \quad (20)$$

$$V_{qs}^* = \left(K_p + K_i \frac{1}{s}\right) (i_{qs}^* - i_{qs}) + \omega_e \sigma L_s i_{ds}^* + \omega_r \frac{L_m}{L_r} \varphi_{rd}. \quad (21)$$

According to the above analysis, the indirect field-oriented control (IFOC) [2, 7, 11] of induction motor with current-regulated PWM drive system can be presented by the block diagram shown in the Fig. 3.

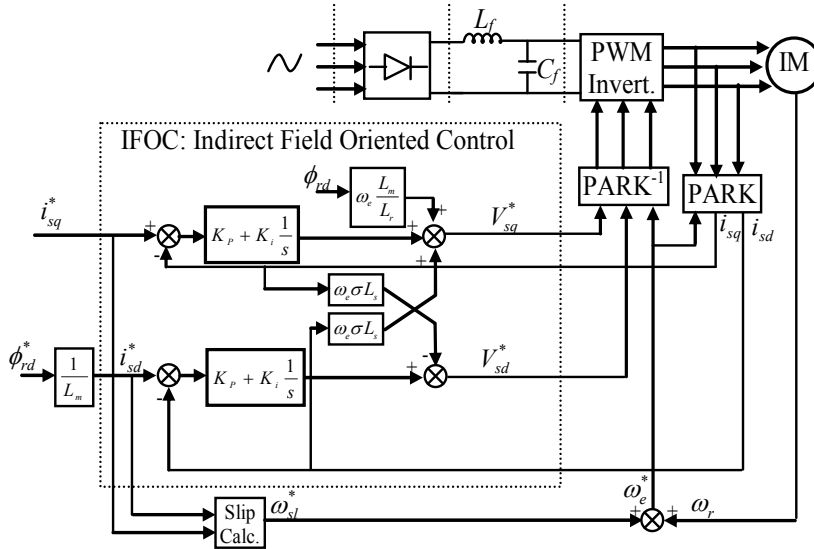


Fig. 3 – Block diagram of IFOC for an induction motor.

#### 4 Sliding Mode Control

A Sliding Mode Controller (SMC) is a Variable Structure Controller (VSC). Basically, a VSC includes several different continuous functions that can map plant state to a control surface, whereas switching among different functions is determined by plant state represented by a switching function [3, 14]. Without loss of generality, consider the design of a sliding mode controller for the following second-order system:  $\ddot{x} + a_1\dot{x} + a_2x = bu$ , where  $u(t)$  is the input to the system and we assume that  $b > 0$ . The following is a possible choice of the structure of a sliding mode controller [2, 6, 11, 14]:

$$u = -k \operatorname{sgn}(s) + u_{eq}, \quad (22)$$

where  $u_{eq}$  stands for equivalent control used when the system state is in the sliding mode [2],  $k$  is a constant, being the maximal value of the controller output.  $s$  is switching function since the control action switches its sign on the two sides of the switching surface  $s = 0$ .  $s$  is defined as [2, 12]:

$$s = e + \lambda e, \quad (23)$$

where  $e = x^* - xe$ ,  $x^*$  being the desired state.  $\lambda$  is a constant,  $\operatorname{sgn}(s)$  is a sign function defined as:

$$\operatorname{sgn}(s) = \begin{cases} -1 & \text{if } s < 0 \\ 1 & \text{if } s > 0 \end{cases} \quad (24)$$

The control strategy adopted here will guarantee the system trajectories move toward and stay on the sliding surface  $s = 0$  from any initial condition if the following condition meets:

$$s \cdot s' \leq -\eta |s|, \quad (25)$$

where  $\eta$  is a positive constant guaranteeing that the system trajectories hit the sliding surface in finite time [2, 3, 6].

Using a sign function often causes chattering in practice. One solution is to introduce a boundary layer around the switch surface [6].

Constant factor  $\phi$  and  $u_s = -k \cdot \text{sat}(s/\phi)$  defines the thickness of the boundary layer.  $\text{sat}(s/\phi)$  is a saturation function defined as:

$$\text{sat}\left(\frac{S}{\phi}\right) = \begin{cases} \frac{S}{\phi}, & \text{if } \left|\frac{S}{\phi}\right| < 1 \\ \text{sgn}\left(\frac{S}{\phi}\right), & \text{if } \left|\frac{S}{\phi}\right| > 1 \end{cases} \quad (26)$$

The diagram of  $u_s$  versus  $s/\phi$  is shown in Fig. 4.

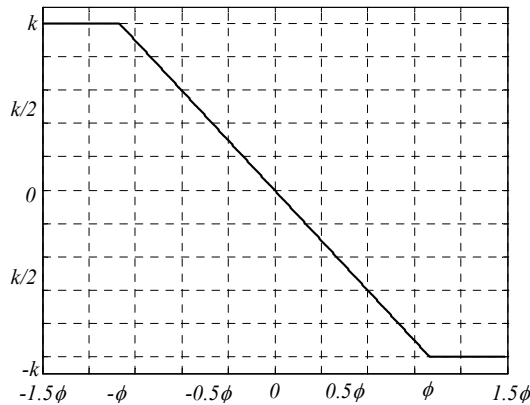


**Fig. 4** – The discontinuous control action of the SMC control law.

#### 4.1 Design of sliding mode current controller

The currents loop is often the inner regulated loop in a field oriented controlled induction motor drive, and the overall performance of the drive depends strongly on the performance of current control. Therefore, a precise and fast current control is essential to achieve high static and dynamic performance for the IFOC of induction motors. If the actual stator currents are not adjusted precisely and instantaneously to the reference values, cross coupling will be

caused between the motor torque and rotor flux. Thus, the performance of the IFOC degrades [3, 14, 15].

In this paper, we propose a current control method based on sliding mode control design. The proposed control design uses two sliding mode controllers to regulate the  $d$ -axis and  $q$ -axis stator currents respectively. The design of the controllers includes two steps.

Firstly, we define sliding surfaces  $s = [s_1 \quad s_2] = 0$  as follows:

$$s_1 = i_{ds}^* - i_{ds} \quad (27)$$

$$s_2 = i_{qs}^* - i_{qs}, \quad (28)$$

where  $i_{ds}^*$  and  $i_{qs}^*$  are the reference values of the  $d$ -axis and  $q$ -axis stator currents, respectively. If the system stays stationary on the surface, then  $s_1 = s_2 = 0$ . Substituting (27) and (28) into  $s_1 = 0$  and  $s_2 = 0$  yields

$$i_{ds} = i_{ds}^* \quad \text{and} \quad i_{qs} = i_{qs}^*. \quad (29)$$

Secondly, we design the voltage control law, which forces the system to move on the sliding surface in a finite time, as follows

$$V_{ds}^* = V_{ds}^{equ} + k_1 \cdot \text{sat}(s_1/\phi_1) \quad (30)$$

$$V_{qs}^* = V_{qs}^{equ} + k_2 \cdot \text{sat}(s_2/\phi_2), \quad (31)$$

where  $V_{ds}^{equ}$  and  $V_{qs}^{equ}$  are the equivalent control actions defined as:

$$V_{ds}^{equ} = \sigma L_s \left( \dot{i}_{ds}^* + \frac{1}{\sigma L_s} \left( R_s + R_r \left( \frac{L_m}{L_r} \right)^2 \right) i_{ds} - \omega_s i_{qs} - \frac{L_m R_r}{\sigma L_s L_r^2} \phi_r^* \right) \quad (32)$$

$$V_{qs}^{equ} = \sigma L_s \left[ \dot{i}_{qs}^* + \omega_s i_{ds} + \frac{1}{\sigma L_s} \left( R_s + R_r \left( \frac{L_m}{L_r} \right)^2 \right) i_{qs} + \frac{L_m}{\sigma L_s L_r} \phi_r^* \omega_m \right] \quad (33)$$

To verify the stability conditions, the parameters  $k_1$  and  $k_2$  must be positives.

#### 4.2 The design of sliding mode speed controller

To control the speed of the induction machine, the sliding surface is defined as follows:

$$s(\omega) = \omega_r^* - \omega_r. \quad (34)$$

The derivative of the sliding surface can be given as:

$$\dot{s}(\omega) = \dot{\omega}_r^* - \dot{\omega}_r. \quad (35)$$

Taking into account the mechanical equation of the induction motor defined in the system of equations (1), the derivative of sliding surface becomes

$$\dot{s}(\omega_m) = \dot{\omega}_m^* - \left( \frac{3}{2} \frac{P^2 L_m \Phi_{dr}^*}{J L_r} i_{qs} - \frac{f_c}{J} \dot{\omega}_m - \frac{P}{J} T_l \right). \quad (36)$$

We take

$$i_{qs} = i_{qs}^{equ} + i_{qs}^n. \quad (37)$$

During the sliding mode and in permanent regime  $s(\omega) = 0$ ,  $\dot{s}(\omega) = 0$  occurs, the equivalent control action being defined as follows:

$$i_{qs}^{equ} = \frac{2}{3} \frac{J L_r}{P^2 L_m \Phi_{dr}^*} \left( \dot{\omega}_m^* + \frac{f_c}{J} \omega_m + \frac{P}{J} T_l \right). \quad (38)$$

The discontinuous control action can be given as:

$$i_{qs}^n = k_{iqs} \cdot \text{sat}(s(\omega)/\phi_\omega). \quad (39)$$

To ensure the system stability the factor  $k_{iqs}$  must be positive.

## 5 Structure of the Studied System

The general scheme of the driving wheels control is represented by Fig. 6. It is an electric vehicle, the wheels of which are controlled independently by two IM. The reference blocks must provide the speed references of each motor taking into consideration information from the different sensors.

### 5.1 Speed references computation

It is possible to determine the speed references versus the requirements of the driver. When the vehicle arrives at the beginning of a curve, the driver applies a curve angle on its wheel [13, 16, 17]. The electronic differential acts immediately on the two motors reducing the driving wheel speed situated inside the curve increasing thereby the speed of the driving wheel outside the curve. The driving wheels angular speeds are as follows:

$$w_{rR} = \frac{V_h}{R_r} + k_b \Delta w \quad (40)$$

$$w_{rL} = \frac{V_h}{R_r} - k_b \Delta w, \quad (41)$$

$k_b = +1$  corresponding to a choice of the direction of the wheel,  $(-1)$  the right turn, and  $(+1)$  the left turn. The driving wheel speed variation is imposed by the trajectory desired by the driver. It is given by:

## Two Wheel Speed Robust Sliding Mode Control for Electric Vehicle Drive

$$\Delta w = \frac{d_w \sin(\delta + \beta) V_h}{2 l_w \cos \delta R_r} \quad (42)$$

The correlation between  $\alpha$  which is the curve angle given by the driver wheel and  $\delta$  of the real curve angle of the wheels is given by:

$$\delta = \frac{\alpha}{k_d} \quad (43)$$

The Fig. 5 shows the vehicle geometry of the studied system.

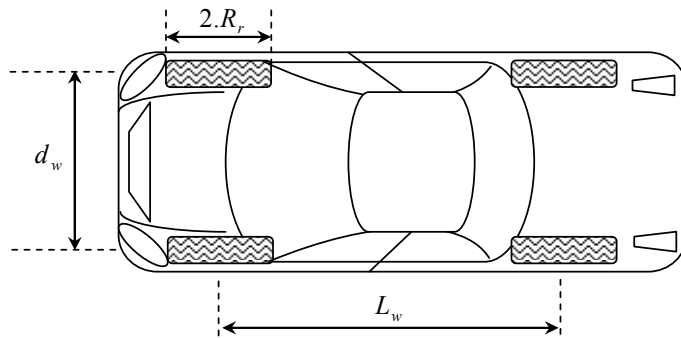


**Fig. 5** – Vehicle geometry,  $k_d$  being the gear ratio;

A proportionality coefficient between  $\delta$  and  $\beta$  (vehicle slip angle) is defined by  $\beta = k\delta$ .

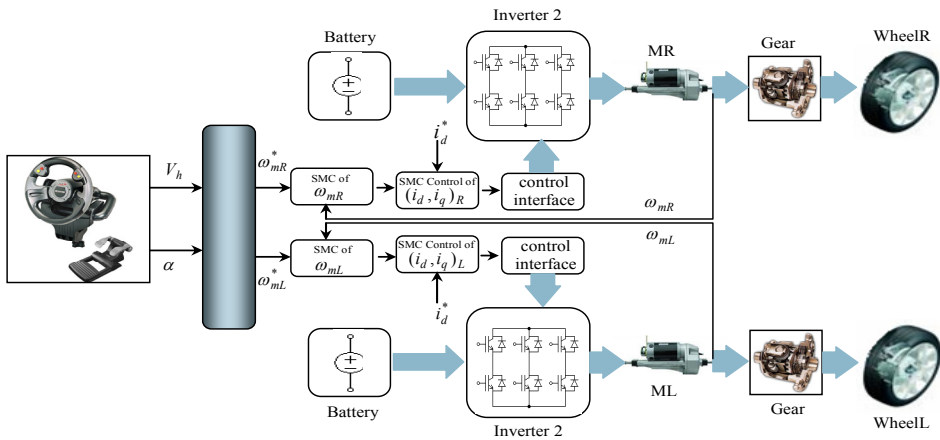


**Fig. 6** – The driving wheels control system.

The speed references of the two motors are:

$$w_{mR}^* = N_{red} w_{rR} \quad (44)$$

$$w_{mL}^* = N_{red} w_{rL} \cdot \quad (45)$$

## 6 Simulation Results

In order to characterise the driving wheel system behaviour, simulations were conducted using the model shown in Fig. 6. They show vehicle speed variation for PI controllers and the sliding mode controller.

In order to simplify the control algorithm and improve the control loop robustness, instead of using classical control, we use the sliding mode control [6]. The advantage of this control is its robustness, its capacity to maintain ideal trajectories independently of the external disturbances and the parameter variations.

To compare the effect of disturbances by resistive torque in the cases of two types of control, Figs. 7a, 7b and 7c shows the system responses in two cases.

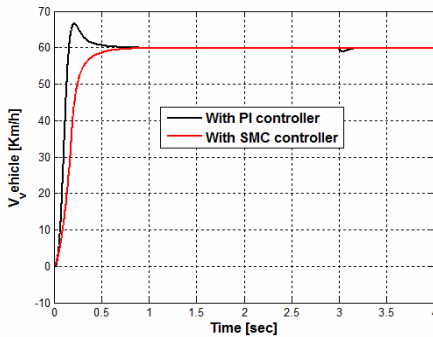


**Fig. 7a** – Vehicle speed for two controller cases

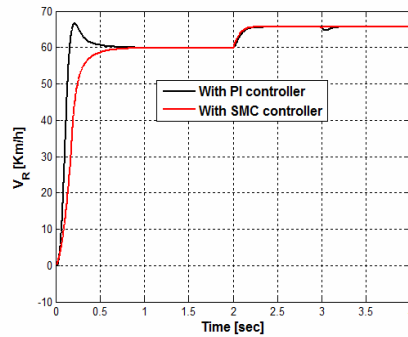


**Fig. 7b** - Right wheel speed in the two cases.

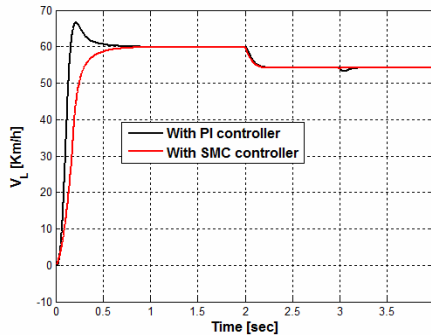


**Fig. 7c** – Left wheel speed in the two cases.

These figures show that the effect of the disturbance is very low in the case of the sliding mode control. It appears clearly that the classical control with PI controller is easy to apply. However the control with sliding mode controllers offers better performances in both control and tracking.

In addition to these dynamic performances, it respects the imposed constraints by the driving system such as the robustness with respect to parameter variations.

**A. Case of straight way**

*Case 1: Flat road with 10% slope at 60km/h speed*

In this test, the system is submitted to the same speed step. The driving wheels speeds stay always the same and the road slope does not affect the control of the wheel. Only a change of the developed motor torque is noticed. The slope effect results in high improvement in the electromagnetic motor torque, both on the left and the right of each motor. The system behaviour is illustrated by Figs. 8a, 8b, 8d, and 8e. Resistive torques are shown in Fig. 8c.

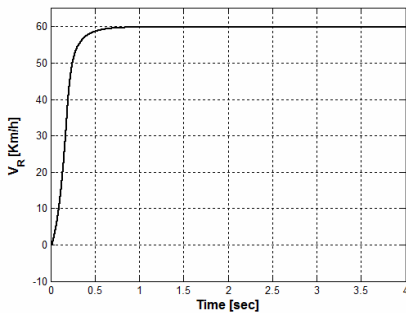


**Fig. 8a** – Right Wheel speed.

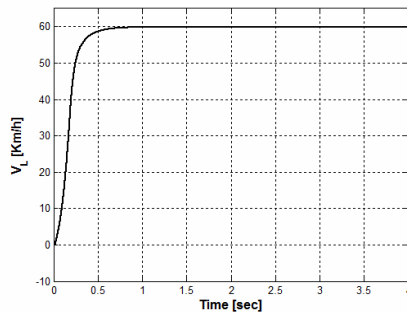


**Fig. 8b** – Left Wheel speed.

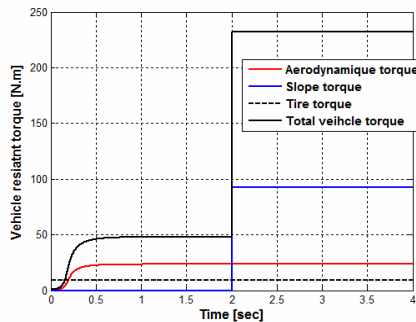


**Fig. 8c** – Resistive Torques.

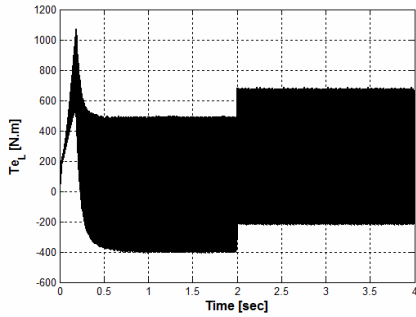


**Fig. 8d** – Left motor Electromagnetic Torque.

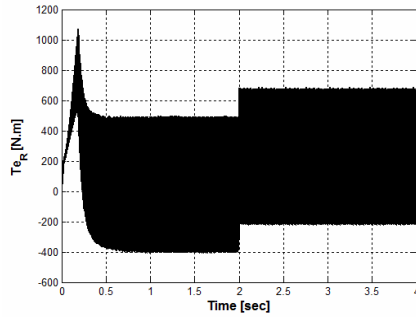


**Fig. 8e** – Right motor Electromagnetic Torque.

### B. Case of curved way

Case1: Curved road on the right at speed of 60km/h

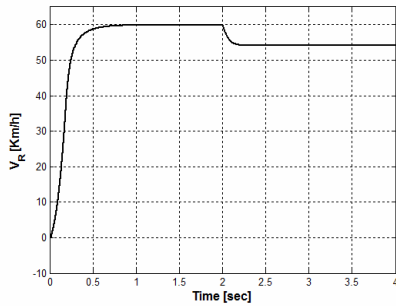


**Fig. 9a** – Right wheel speed.

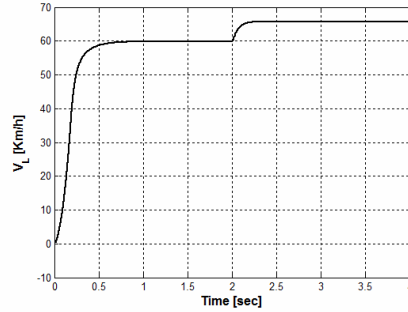


**Fig. 9b** – Left wheel speed.

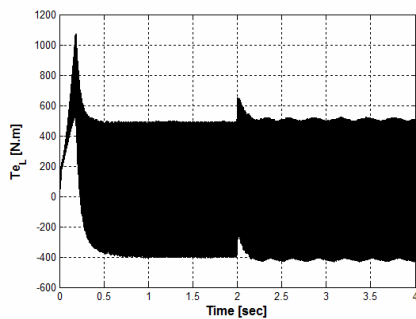


**Fig. 9c** – Left motor Electromagnetic Torque.

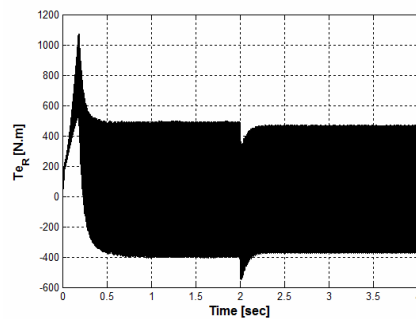


**Fig. 9d** – Right motor Electromagnetic Torque.

## Two Wheel Speed Robust Sliding Mode Control for Electric Vehicle Drive

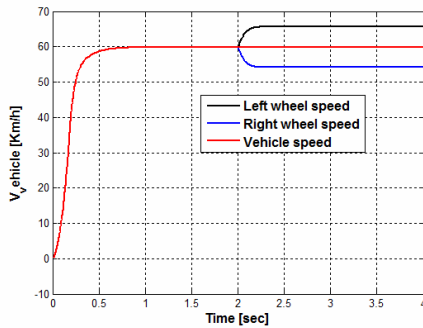


**Fig. 9e** – *Vehicle speed in right turn in curved way.*

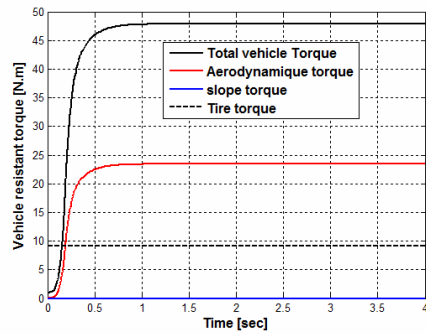


**Fig. 9f** – *Resistive Torques in right turn in curved way.*

The vehicle is driving on a curved road on the right side with 60km/h speed. The assumption is that the two motors are not disturbed. In this case the driving wheels follow different paths, and they turn in the same direction but with different speeds.

The electronic differential acts on the two motor speeds by decreasing the speed of the driving wheel on the right side situated inside the curve, and on the other hand by increasing the wheel motor speed in the external side of the curve. The behaviour of these speeds is given by Figs. 9a, 9b and 9c.

### *Case 2: Curved road with 10% slope with left turn*

This test shows the influence of the road slope on the vehicle moving in curved road. Figs. 10a, 10b, 10c, 10d, 10e and 10f shows the effect of the slope and the curved road on the motor parameters. The driving wheels speeds are controlled and the errors created by the disturbances are quickly compensated.

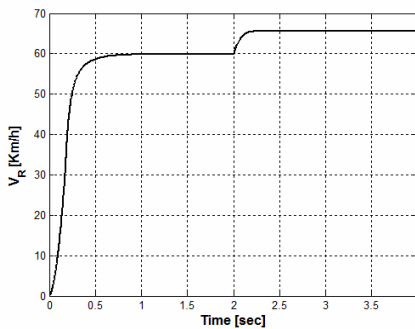


**Fig. 10a** – *Right Wheel speed.*

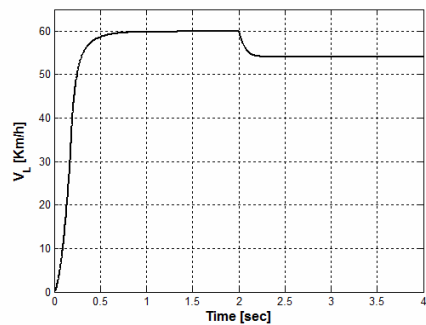


**Fig. 10b** – *Left Wheel speed.*

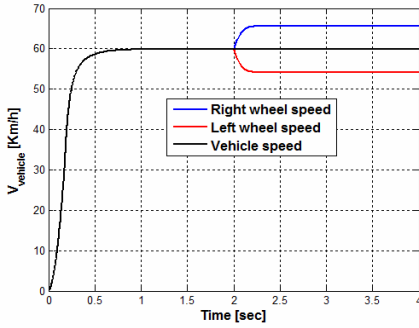


**Fig. 10c** – Vehicle speed in left turn curved way.

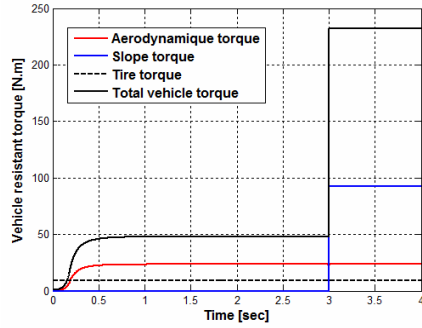


**Fig. 10d** – Resistive Torques in left turn curved way.

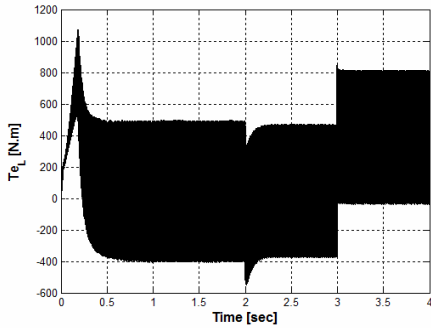


**Fig. 10e** – Left motor Electromagnetic Torque left turn curved way.

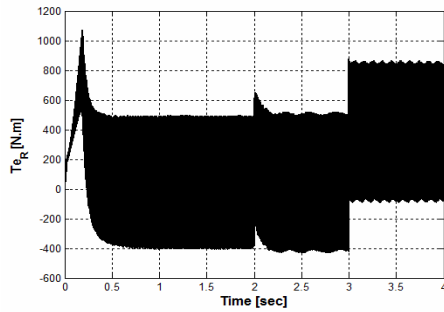


**Fig. 10f** – Right motor Electromagnetic Torque left turn curved way.

## 7 Conclusion

In the field of electric drives with variable speed, an application of an electric vehicle controlled by an electronic differential is presented. This paper proposes an ‘independent machine’ control structure applied to a propulsing system by the sliding mode speed control. The results obtained by the simulation show that this structure provides the realization of the robust control based on Lyapunov switching area and ensures good dynamic and static performance.

The proposed sliding mode model controls the driving wheels speed with high accuracy either in flat roads or curved ones giving real estimations of the stator quadratic current in each case. The disturbances do not affect the performance of the driving motors.

## 9 References

- [1] A. Bouscayrol, B. Davat, B. François, J.P., Hautier, F. Meibody-Tabar, M., Pietrzak-David: Multimachine Multiconverter Systems: Application to Electromechanical Drives, EPJ Applied Physics, Vol. 10, No. 2, May 2000, pp. 131 – 147.
- [2] L. Baghli: Contribution to Induction Machine Control: Using Fuzzy Logic, Neural Networks and Genetic Algorithms, Doctoral Thesis (in French), Henri Poincare University, January 1999.
- [3] M.A. Ouhrouche, C. Volet: Simulation of a Direct Field-Oriented Controller for an Induction Motor Using Matlab/Simulink Software Package, Proc. of IASTED Int. Conf. Modeling and Simulation, USA, 2000.
- [4] F. Chabrot: Contribution à la conception d'un entraînement basé sur une machine à aimants permanents fonctionnant sans capteur sur une large plage de vitesse: Application au véhicule électrique. (Contribution to the Conception of a Training Based on Permanent Magnets Synchronous Machine Operating without Sensor on a wide Range of Speed: Application to the Electric Vehicle) Thèse de doctorat (Doctorat thesis). INP de TOULOUSE, Jan. 2000.
- [5] B. Multon, L. Hirsinger: Problème de la motorisation d'un véhicule Electrique (Motorization Problem of an Electric Vehicle), EEA "Voiture et Electricité" ("Car and Electricity"), Cachan, France, 24 et 25 Mars 1994.
- [6] J. Jung, K. Nam: A Dynamic Decoupling Control Scheme for High-Speed Operation of Induction Motors, IEEE Trans. on Ind. Elect., Feb. 1999, Vol. 46, No. 1, pp. 100 – 110.
- [7] M. Zhiwen, T. Zheng, F. Lin, X. You: A New Sliding-Mode Current Controller for Field Oriented Controlled Induction Motor Drives, IEEE Int. Conf. IAS, Nov. 2005, pp. 1341 – 1346.
- [8] H. Yoichi, T. Yasushi, T. Yoshimasa: Traction Control of Electric Vehicle: Basic Experimental Results using the Test EV, "UOT Electric march", IEEE. Transactions on Industry Applications, September/October 1998, Vol. 34, No. 5, pp. 1131 – 1138.
- [9] S. Sadeghi, J. Milimonfared, M. Mirsalim, M. Jalalifar: Dynamic Modeling and Simulation of a Switched Reluctance Motor in Electric Vehicle, Proc ICIEA Conf, 2006.
- [10] A. Hazzab, I.K. Bousserhane, M. Kamli, M. Rahli: New Adaptive Fuzzy PI-Sliding Mode Controller for Induction Machine Speed Control, Third IEEE International Conference on Conference on Systems, Signals & Devices SSD'05, Tunisia, 2005.
- [11] Derdiyok, M. K. Guven, H. Rahman, N. Inane, L. Xu: Design and Implementation of New Sliding-Mode Observer for Speed-Sensorless Control of Induction Machine, IEEE Trans. on Industrial Electronics, Vol. 49, No. 5, Oct. 2002, pp. 1177 – 1182.
- [12] C.E. Barbier, B. Negarede, H.L Meyer: Global Control Strategy Optimization of an Asynchronous Drive System for an Electric Vehicle, Control Eng. Practice, Vol. 4, No. 8, Aug. 1996, pp. 1053 – 1066.
- [13] J. Larminie, J. Lowry: Electric Vehicle Technology Explained, John Wiley & Sons, England, 2003.
- [14] R.J. Wai: Adaptive Sliding-Mode Control for Induction Servomotor Drives, IEE Proc. Electr. Power Appl., Vol. 147, No. 6, Nov. 2000, pp. 553 – 562.
- [15] C.M. Lin, C.F. Hsu: Adaptive Fuzzy Sliding-Mode Control for Induction Servomotor Systems, IEEE Transactions on Energy Conversion, Vol. 19, No. 2, June 2004, pp. 362 – 368.
- [16] M. Ehsani, K.M. Rahman, H.A. Toliyat: Propulsion System Design of Electric and Hybrid Vehicle, IEEE Tran. on Industrial Electronics, Vol. 44, No.1, Feb. 1997, pp. 19 – 27.

- [17] H. Huang: Electrical Two Speed Transmission and Advanced Control of Electric Vehicles, Doctoral Thesis, New Brunswick University, June 1998.
- [18] J.C. Lo, Y.H. Kuo: Decoupled Fuzzy Sliding-mode Control, IEEE Trans. on Fuzzy Systems, Vol. 6, No. 3, 1998, pp. 426 – 435.

## Appendix

**Table 1**  
*Electric vehicle Parameters.*

$T_e$	Motor traction torque	247 Nm
$J_e$	Moment on inertia of the drive train	7.07Kgm <sup>2</sup>
$R_w$	Wheel radius	0.36m
$a$	Total gear ratio	10.0
$\eta$	Total transmission efficiency	0.93
$M$	Vehicle mass	3904Kg
$f_e$	Bearing friction coefficient	0.001
$K_d$	Aerodynamic coefficient	0.46
$A$	Vehicle frontal area	3.48 m <sup>2</sup>
$f_v$	Vehicle friction coefficient	0.01
$\alpha$	Grade angle of the road	rad
$L_w$	Distance between two wheels and axes	2.5m
$d_w$	Distance between the back and the front wheel	1.5m

**Table 2**  
*Induction Motors Parameters.*

$R_r$	Rotor winding resistance (per phase)	0.003 $\Omega$
$R_s$	Stator winding resistance (per phase)	0.0044 $\Omega$
$L_s$	Stator leakage inductance (per phase)	16.1 $\mu$ H
$L_m$	Magnetizing inductance (per phase)	482 $\mu$ H
$L_r$	Rotor leakage inductance (per phase)	12.9 $\mu$ H
$f_c$	Friction coefficient	0.0014
$P$	Number of poles	4
	Based speed	2885 rpm
	Rated power	100 hp